Articles

Titanium(IV) Alkoxy-N-heterocyclic Carbenes: Structural Preferences of Alkoxide and Bromide Adducts

Shaheed A. Mungur, Alexander J. Blake, Claire Wilson, Jonathan McMaster, and Polly L. Arnold*

School of Chemistry, University of Nottingham, University Park, Nottingham, NG7 2RD, U.K.

Received October 14, 2005

A series of titanium(IV) adducts of an amido-tethered N-heterocyclic carbene (NHC) of the form $Ti(L)(O^iPr)_n(Br)_{3-n}$ ($n = 1-3$, L = ^{t}BuNHCH$_2$CH$_2$[C{N^{t}Bu(CHCH)N}]) have been synthesized and characterized. Structural characterization of the $n = 2$ complex shows marked bending of the two ligands *cis* (and perpendicular) to the plane of the NHC group in the direction of the carbene, suggestive of a pseudo-back-bonding interaction between adjacent ligands and the carbene p orbital, consistent with a bonding model recently proposed for d^0 metal-NHC complexes. However, inspection of a space-filling model and the calculation of bond order using DFT methods suggest that the bending is due to repulsions between lone pairs on the adjacent π-donor ligands in the complexes and not any specific interaction between the NHC and *cis* π-donor ligands.

Introduction

The diversity of NHC (N-heterocyclic carbene) ligands found in late transition metal chemistry and homogeneous catalysis is conspicuously absent in early transition metal NHC systems; until recently, the majority of early metal complexes reported were symmetrical N,N′-alkyl-substituted NHC adducts such as $TiCl_4(C\{N^iPrCMe\}_2\}$.[1−3] However, an increasing number of catalyst systems that combine one of the more Lewis acidic metals and an NHC are being described. For example, homogeneous catalytic systems that incorporate an NHC have been used to modify the activity of reactions, including catalysts for D,L-lactide polymerization,[4] methyl methacrylate polymerization,[5] epoxide alkylation,[6] and alkene polymerization.[7,8] Some high-oxidation-state transition metal NHC complexes, for example $V(O)Cl_3(C\{NMesCH\}_2)$ (Mes = mesityl)[9] and $ReNCl_2(PMe_2Ph)_2(L^1)$] (L^1 = 1,3,4-triphenyl-1,2,4-triazol-5-ylidene),[10] also display exceptional stability to air and moisture compared with the non-NHC-containing analogues.

Chart 1

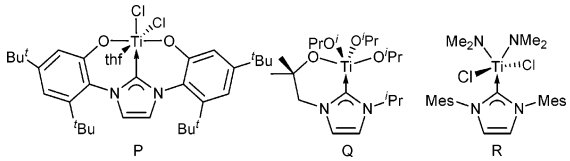

It is possible to enhance the binding of the NHC to more electropositive metals by the incorporation of chelating anionic groups into the N-alkyl sidearms, such as aryloxide, exemplified by **P**, Chart 1,[11−13] and we have been pursuing this approach by preparing asymmetrically substituted, functionalized bidentate NHCs as ligands for s-, d-, and f-block metal cations.[14−17] These complexes exploit the hemilabile reactivity of the carbene in **Q**, Chart 1, affording a new catalyst for lactide polymerization.[18]

We have recently noted a number of electrostatic interactions of the form η^1- or η^2-NHC···K$^+$, involving the π-electrons

* To whom correspondence should be addressed. Fax: 44 115 9513563. Tel: 44 115 9513437. E-mail: polly.arnold@nottingham.ac.uk.

(1) Kuhn, N.; Kratz, T.; Blaser, D.; Boese, R. *Inorg. Chim. Acta* **1995**, 238, 179−181.
(2) Alder, R. W.; Blake, M. E.; Chaker, L.; Harvey, J. N.; Paolini, F.; Schutz, J. *Angew. Chem., Int. Ed.* **2004**, *43*, 5896.
(3) Alder, R. W.; Blake, M. E.; Bortolotti, C.; Bufali, S.; Butts, C. P.; Linehan, E.; Oliva, J. M.; Orpen, A. G.; Quayle, M. J. *Chem. Commun.* **1999**, 241−242.
(4) Jensen, T.; Breyfogle, L.; Hillmyer, M.; Tolman, W. *Chem. Commun.* **2004**, 2504.
(5) Glanz, M.; Dechert, S.; Schumann, H.; Wolff, D.; Springer, J. *Z. Anorg. Allg. Chem.* **2000**, *626*, 2467−2477.
(6) Zhou, H. Y.; Campbell, E. J.; Nguyen, S. T. *Org. Lett.* **2001**, *3*, 2229−2231.
(7) Niehues, M.; Erker, G.; Kehr, G.; Schwab, P.; Frohlich, R.; Blacque, O.; Berke, H. *Organometallics* **2002**, *21*, 2905−2911.
(8) McGuinness, D. S.; Gibson, V. C.; Steed, J. W. *Organometallics* **2004**, *23*, 6288−6292.
(9) Abernethy, C. D.; Codd, G. M.; Spicer, M. D.; Taylor, M. K. *J. Am. Chem. Soc.* **2003**, *125*, 1128−1129.
(10) Abram, H. B. a. U. *Chem. Commun.* **2003**, 2436.
(11) Arnold, P. L.; Scarisbrick, A. C.; Blake, A. J.; Wilson, C. *Chem. Commun.* **2001**, 2340−2341.
(12) Aihara, H.; Matsuo, T.; Kawaguchi, H. *Chem. Commun.* **2003**, 2204−2205.
(13) Spencer, L. P.; Winston, S.; Fryzuk, M. D. *Organometallics* **2004**, *23*, 3372−3374.
(14) Arnold, P. L.; Mungur, S. A.; Blake, A. J.; Wilson, C. *Angew. Chem., Int. Ed.* **2003**, *42*, 5981−5984.
(15) Arnold, P. L.; Rodden, M.; Davis, K. M.; Scarisbrick, A. C.; Blake, A. J.; Wilson, C. *Chem. Commun.* **2004**, 1612−1613.
(16) Liddle, S. T.; Arnold, P. L. *Organometallics* **2005**, *24*, 2597.
(17) Arnold, P. L.; Blake, A. J.; Wilson, C. *Chem. Eur. J.* **2005**, *11*, 6095.
(18) Patel, D.; Liddle, S. T.; Mungur, S. A.; Rodden, M.; Blake, A. J.; Arnold, P. L. *Chem. Commun.* **2006**, 1124.

10.1021/om0508839 CCC: $33.50
Publication on Web 03/16/2006

of the NHC, in the solid-state molecular structure of the aggregated potassium alkoxide carbene [{K[$OCMe_2CH_2$-(1-C{NCHCHN^{i}Pr})]}$_8$(thf)]$_\infty$.[19] Conversely, η^1-NHC interactions between the (formally empty) carbenic carbon p orbital and the lone pairs of an adjacent chloride, possibly though an empty t_{2g} orbital of the metal cation, have also been identified in two closed-shell, d^0 metal NHC complexes: Ti(NMe_2)$_2$-(C{NMesCH}$_2$)Cl_2, **R**,[20] and the related d^0 vanadium complex V(O)Cl_3(C{NMesCH}$_2$) (Mes = mesityl).[9] This orbital interaction is proposed to account for the acute angle between the NHC and the halide ligand measured in the solid-state crystal structures of each complex (mean 83.3° and 81.6°, respectively).

Herein, we report a series of new titanium(IV) adducts of an amido-functionalized NHC, Ti(L)(O^iPr)$_n$(Br)$_{3-n}$ (n = 1−3, L = ^{t}BuNHCH_2CH_2[C{N^{t}Bu(CHCH)N}]), and a related *tert*-butyl imidazole adduct, [Ti(L)(O^iPr)$_2$($NC_3H_3N(^t$Bu)]Br. The structurally characterized adducts display distortions away from trigonal bipyramidal toward square-based pyramidal geometries and an acute angle between the NHC and the halide ligand; we discuss the factors that may account for the observed geometries in these complexes.

Experimental Details

2.1. General Methods. All manipulations were carried out using standard Schlenk techniques or an MBraun UniLab glovebox under an atmosphere of dry dinitrogen. Hexane, toluene, THF, and diethyl ether were dried by passage through activated alumina towers and were degassed before use. Benzene was distilled from potassium under an atmosphere of dry dinitrogen. All solvents were stored over potassium mirrors (with the exception of THF, which was stored over activated 4 Å molecular sieves). Deuterated solvents were distilled from potassium, degassed by three freeze−pump−thaw cycles, and stored under dinitrogen. Chlorotitanium tris(isopropoxide) was purchased from Aldrich and recrystallized before use. The compounds [HL·LiBr] and 1-*tert*-butyl-1*H*-imidazole[14] were prepared by published literature procedures.

^{1}H and ^{13}C{^{1}H} NMR spectra were recorded on a Bruker 300 spectrometer operating at 300.1 and 75.5 MHz, respectively; chemical shifts are quoted in ppm and are relative to $SiMe_4$. Elemental microanalyses were carried out by Mr. Stephen Boyer at the Microanalysis Service, London Metropolitan University, UK.

2.2. Preparations. 2.2.1. [LiL]·LiBr, 1. To a cooled solution (−78 °C) of HL·LiBr (5.00 g, 13 mmol) in thf (10 mL) was added 1.6 M *n*-BuLi (8 mL, 1 equiv). The solution was allowed to warm to room temperature and stirred for 18 h. The resultant peach-colored solution was filtered, and the volatiles were removed under reduced pressure to yield **1** as a colorless solid (4.01 g, 99.8%). ^{1}H NMR (300 MHz, d_6-benzene, 298 K): δ 6.44 (s, 1H, CH), 6.30 (s, 1H, CH), 4.00 (bs, 2H, CH_2), 3.48 (bs, 2H, CH_2), 1.43 (s, 9H, *t*Bu), 1.33 (s, 9H, *t*Bu).

2.2.2. [LiL]·2LiBr, 1a. To a cooled suspension (−78 °C) of [H_2L]Br_2 (0.50 g, 1.3 mmol) in thf (10 mL) was added 1.6 M *n*-BuLi (2.44 mL, 3.9 mmol, 3 equiv, 10 mL). The pearly cream slurry was allowed to warm to room temperature and stirred for 48 h. Volatiles were removed under reduced pressure from the resultant off-white solution to yield [LiL]·2LiBr as a very pale yellow powder (0.458 g, 89%). The pearly, colorless solid is insoluble in benzene, but addition of a drop of dilute aqueous HBr quantitatively regenerates the ligand [H_2L]Br_2 as observed by ^{1}H NMR spectroscopy in $CDCl_3$.

2.2.3. Ti(L)(O^iPr)$_3$, 2. To a solution of [TiCl(O^iPr)$_3$] (2.6 g, 10 mmol) in thf (5 mL) was added a solution of HL (2.29 g, 10 mmol) in thf (5 mL). The solution immediately turned yellow and was allowed to stir for a further 18 h. The suspension was filtered to leave a yellow solid, which was extracted with diethyl ether and combined with the toluene filtrate. The volatiles from the combined filtrates were removed under reduced pressure to isolate **2** as a yellow oil (0.77 g, 17.2%). ^{1}H NMR (300 MHz, d_6-benzene, 298 K): δ 1.30 (s, 9H, *t*Bu), 1.33 (d, $^3J_{HH}$ = 3.9 Hz, 18H, 3 × *i*Pr), 1.53, (s, 9H, *t*Bu), 3.69 (t, $^3J_{HH}$ = 7.3 Hz, 2H, CH_2), 4.34 (t, $^3J_{HH}$ = 7.3 Hz, 2H, CH_2), 4.73 (sept., $^3J_{HH}$ = 6.1 Hz, 3H, 3 × $CHMe_2$), 6.60 (d, $^3J_{HH}$ = 1.5 Hz, 1H, CH), 6.62 (d, $^3J_{HH}$ = 1.5 Hz, 1H, CH). ^{13}C{^{1}H} NMR (75 MHz, d_6-benzene, 298 K): δ 25.01 (*i*Pr), 28.40 (*t*Bu), 28.30 (*t*Bu), 49.84 (CH_2), 51.78 (CMe_3), 54.28 (CMe_3), 56.17 (CH_2), 74.07 ($CHMe_2$), 113.06 (CH), 116.09 (CH), 205.58 ($C_{carbene}$).

2.2.4. Ti(L)(O^iPr)$_2$Br, 3. A solution of [TiCl(O^iPr)$_3$] (1.17 g, 4.5 mmol) in toluene (10 mL) was added to a suspension of [LiL·LiBr], **1** (1.43 g, 4.5 mmol), in toluene (10 mL). The solution was stirred for 18 h during which the solution turned yellow. The mixture was filtered and the volatiles were removed from the filtrate to afford a yellow oil. Diethyl ether (5 mL) was added and the solution cooled (−30 °C); after standing overnight, **3** was recovered as a crystalline yellow solid (0.65 g, 30%). ^{1}H NMR (300 MHz, d_6-benzene, 298 K): δ 1.36 (d, $^3J_{HH}$ = 4.0 Hz, 12H, 2 × *i*Pr), 1.43 (s, 9H, *t*Bu), 1.47(s, 9H, *t*Bu), 3.48 (bs, 2H, CH_2), 3.90 (bs, 2H, 2 × $CHMe_2$), 5.29 (bs, 2H, CH_2), 6.04 (d, $^3J_{HH}$ = 1.2 Hz, 1H, CH), 6.35 (d, $^3J_{HH}$ = 6.27 Hz, 1H, CH). ^{13}C{^{1}H} NMR (75 MHz, d_6-benzene, 298 K): δ 23.64, (*t*Bu), 28.28 (*t*Bu), 28.73 (*i*Pr), 49.47 ($CHMe_2$), 51.81 ($CHMe_2$), 56.44 (CH_2), 62.97 (CH_2), 75.30 (CMe_3), 80.66 (CMe_3), 115.28 (CH), 118.60 (CH), 187.57 ($C_{carbene}$). Anal. Found: C 48.54, H 8.01, N 9.06. Calc for $C_{19}H_{38}BrN_3O_2Ti$: C 48.73, H 8.18, N 8.97.

2.2.5. Ti(L)(O^iPr)Br_2, 4. To a cooled (−78 °C) suspension of [LiL·2LiBr] (1.5 g, 3.9 mmol) in thf (20 mL) was added 2.5 M ^{n}BuLi (4.67 mL). The suspension was allowed to warm to room temperature and was stirred for a further hour. The volatiles were removed under reduced pressure, and to the resulting solid were added [TiCl(O^iPr)$_3$] (1.01 g, 3.9 mmol) and thf (10 mL). The solution was allowed to stir for a further 18 h, after which volatiles were removed under reduced pressure. The yellow solid was extracted into diethyl ether. Concentration and cooling of the solution to −30 °C afforded a crop of **4** as a yellow solid (0.33 g, 17.4%). ^{1}H NMR (300 MHz, d_5-pyridine, 298 K): δ 1.26 (*t*Bu), 1.38 (d, 6H, $^3J_{HH}$ = 6.1 Hz, 2 × CH_3), 1.64 (*t*Bu), 3.75 (t, $^3J_{HH}$ = 7.2 Hz, 2H, CH_2), 4.44 (t, $^3J_{HH}$ = 7.2 Hz, 2H, CH_2), 4.93 (bs (unresolved sept.), 1H, $CHMe_2$), 7.14 (s, 1H, CH), 7.20 (s, 1H, CH). Anal. Found: C 39.49, H 6.40, N 8.48. Calc for $C_{16}H_{31}Br_2N_3OTi$: C 39.29, H 6.39, N 8.59.

2.2.6. Ti(L)(O^iPr)$_2$(tBuimz), 5. To 1-*tert*-butyl-1*H*-imidazole (100 mg, 0.21 mmol) was added a solution of **3** (26.4 mg, 0.21 mmol) in d_6-benzene (0.55 mL). The mixture was shaken and left standing for 2 h. The yellow solution was analyzed by ^{1}H NMR spectroscopy. ^{1}H NMR (300 MHz, d_6-benzene, 298 K): δ 7.49 (s, 1H, CH), 7.33 (s, 1H, CH), 6.62 (s, 1H, CH), 6.31 (s, 1H, CH), 6.10 (s, 1H, CH), 5.30 (bs, 2H, CH_2), 3.90 (bs (unresolved sept.), 2H, $CHMe_2$), 3.43 (bs, 2H, CH_2), 1.46 (s, 9H, *t*Bu), 1.43 (s, 9H, *t*Bu), 1.37 (bd, 12H, *i*Pr), 0.91 (s, 9H, *t*Bu).

2.3. Crystallography. Crystal data for the structures are collected in Table 1. Crystals were examined on an Apex CCD area detector diffractometer using graphite-monochromated Mo Kα radiation (λ = 0.71073 Å) at 150(2) K. Intensities were integrated from data recorded on narrow (0.3°) frames by ω rotation. Cell parameters were refined from the observed positions of all strong reflections in each data set. Semiempirical absorption corrections were applied based on symmetry-equivalent and duplicate reflections. The structures were solved by direct methods and were refined

(19) Arnold, P. L.; Rodden, M.; Wilson, C. *Chem. Commun.* **2005**, 1743.
(20) Shukla, P.; Johnson, J. A.; Vidovic, D.; Cowley, A. H.; Abernethy, C. D. *Chem. Commun.* **2004**, 360−361.

Table 1. Crystal Experimental Details

	compound **3** (containing A and B)	compounds **3**, **5** (containing C and D)
	Crystal Data	
chemical formula	$C_{19}H_{38}BrN_3O_2Ti$	$C_{24.50}H_{49}BrN_4O_{2.50}Ti$
M_r	468.33	567.49
cell setting, space group	monoclinic, $P2_1/c$	triclinic, $P\bar{1}$
a, b, c (Å)	16.539 (3), 27.592 (5), 10.484 (2)	11.9167 (12), 16.839 (2), 17.300 (2)
α, β, γ (deg)	90.00, 91.234 (3), 90.00	86.068 (2), 78.108 (2), 70.852 (2)
V (Å^3)	4783 (2)	3209.1 (10)
Z	8	4
D_x (Mg m^{-3})	1.301	1.175
no. of reflns for cell params	5389	4003
θ range (deg)	2.4−25.5	2.4−22.6
μ (mm^{-1})	2.04	1.54
cryst form, color	lath, colorless	tablet, colorless
cryst size (mm)	0.68 × 0.20 × 0.06	0.35 × 0.31 × 0.13
	Data Collection	
T_{min}	0.720	0.722
T_{max}	1.000	1.000
no. of measd, indep and obsd params	28 905, 10 964, 7804	22 778, 11 241, 7386
criterion for obsd reflns	$I > 2\sigma(I)$	$I > 2\sigma(I)$
R_{int}	0.049	0.044
θ_{max} (deg)	27.5	25.0
range of h, k, l	$-21 \rightarrow h \rightarrow 18$ $-35 \rightarrow k \rightarrow 35$ $-13 \rightarrow l \rightarrow 10$	$-14 \rightarrow h \rightarrow 14$ $-20 \rightarrow k \rightarrow 20$ $-19 \rightarrow l \rightarrow 20$
	Refinement	
refinement on	F^2	F^2
$R[F^2 > 2\sigma(F^2)]$, $wR(F^2)$, S	0.052, 0.137, 1.02	0.064, 0.191, 1.02
no. of reflns	10 964	11 241
no. of params	469	561
weighting scheme	calcd $w = 1/[\sigma^2(F_o^2) + (0.065P)^2 + 4.983P]$ where $P = (F_o^2 + 2F_c^2)/3$	calcd $w = 1/[\sigma^2(F_o^2) + (0.091P)^2 + 6.321P]$ where $P = (F_o^2 + 2F_c^2)/3$
$(\Delta/\sigma)_{max}$	0.001	0.001
$\Delta\rho_{max}$, $\Delta\rho_{min}$ (e Å^{-3})	0.85, −0.87	0.94, −0.55

by least-squares methods on all unique F^2 values, with anisotropic displacement parameters, and with constrained riding hydrogen geometries; U(H) was set at 1.2 (1.5 for methyl groups) times U_{eq} for the parent atom. The largest features in the final difference Fourier syntheses were close to heavy atoms. Computer programs used were Bruker SMART (control) and SAINT (integration),[21] and SHELXTL for structure solution, refinement, and molecular graphics.[22]

2.3.1. Theoretical Calculations. Spin-restricted geometry optimization calculations of **3** were performed using the Amsterdam Density Functional (ADF) suite version 2003.01.[23−25] These calculations employed a Slater-type orbital (STO) triple-ζ plus one polarization function basis set from the TZP database of the ADF suite for all atoms. Frozen core basis sets (up to and including 3d for Br, 3p for Ti, and 1s for C, N, O) were employed. The local density approximation (LDA) with the correlation potential due to Vosko et al.[26] was used in all of the DFT calculations. Gradient corrections were performed using the functionals of Becke[27] and Perdew (BP).[28] A model of **3** was constructed using geometrical data from the X-ray crystal structure of **3**, and the geometry was optimized without any constraints. The atom-numbering schemes and the coordinate frames employed in the calculations are shown in Figure 3.

Scheme 1

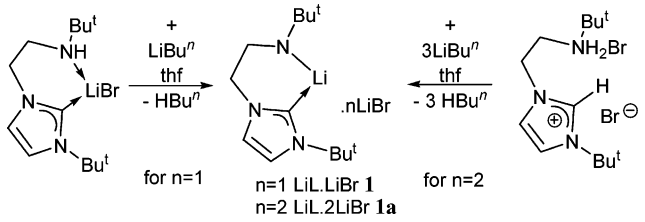

Wiberg bond order indices[29] between fragments of **3** were calculated using AOMix-L Revision 1.38[30] from the results of single-point ADF calculations, using an all-electron basis set from the TZP database, on structures geometry-optimized as above.

Results and Discussion

The treatment of the lithium bromide-stabilized aminocarbene ^{t}BuNHCH$_2$CH$_2$[C{N^{t}Bu(CHCH)N}]·LiBr with 1 equiv of *n*-butyllithium, or the proligand ^{t}BuNH$_2$CH$_2$CH$_2$[HC{N^{t}Bu-(CHCH)N}]2Br, [H$_3$L]Br$_2$, with 3 equiv of *n*-butyllithium in thf affords the lithium amido-carbenes [LiL]·LiBr (**1**) and [LiL]·2LiBr (**1a**), respectively, both of which incorporate lithium bromide from the starting materials,[14] Scheme 1. The incorporation of lithium bromide with **1** and **1a** presumably results from the combination of the solubility of lithium bromide in thf and the donor strength of the NHC pair; the crystal structures of the previously reported [HL]·LiBr and [HL]·2LiBr contain a combination of Li−C$_{carbene}$, Li−N, and Li−Br dative bonds.[14] This salt incorporation attenuates the reactivity of the

(21) Bruker *SMART and SAINT*; Bruker AXS Inc.: Madison, WI, 2001.
(22) Sheldrick, G. M. *SHELXTL v. 6.12*; Bruker AXS Inc.: Madison, WI, 2001.
(23) Fonseca Guerra, C.; Snijders, J. G.; te Velde, G.; Baerends, E. J. *Theor. Chem. Acc.* **1998**, *99*, 391.
(24) *SCM*; Vrije Universiteit Amsterdam; http://www.scm.com, Amsterdam, The Netherlands.
(25) te Velde, G.; Bickelhaupt, F. M.; van Gisbergen, S. J. A.; Fonseca Guerra, C.; Baerends, E. J.; Snijders, J. G.; Ziegler, T. *J. Comput. Chem.* **2001**, *22*, 931−967.
(26) Vosko, S. H.; Wilk, L.; Nusair, M. *Can. J. Phys.* **1980**, *58*, 1200.
(27) Becke, A. D. *Phys. Rev. A* **1988**, *38*, 3098.
(28) Perdew, J. P. *Phys. Rev. B* **1986**, *33*, 8822.
(29) Wiberg, K. B. *Tetrahedron* **1968**, *24*, 1083.
(30) Gorelsky, S. I.; Lever, A. B. P. *J. Organomet. Chem.* **2001**, *635*, 187.

Scheme 2

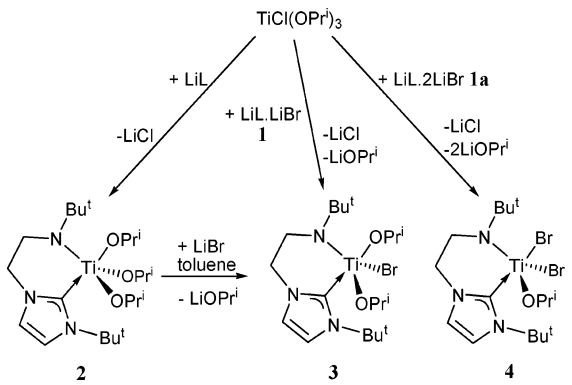

carbene, so **1** is a relatively air-stable, light-stable pale yellow powder, which is significantly easier to manipulate than AgL (which is light sensitive)[31] or LiL (which is extremely air sensitive).[14]

Several lithium(I) NHC complexes have now been prepared, using suitable counteranions such as cyclopentadienide; these all generally appear to be stable crystalline solids that are readily handled in an inert atmosphere.[14,15,32]

A solution of LiL in toluene was added to a cooled (−78 °C) solution of TiCl(O^{i}Pr)$_3$ in toluene, and the yellow solution was allowed to warm to room temperature over 18 h. After filtration and removal of volatiles from the filtrate, a yellow oil was isolated in poor yield and characterized as Ti(L)(O^{i}Pr)$_3$ **2** (17%). The $^{13}C\{^1H\}$ NMR spectrum of **2** contains one high-frequency resonance attributed to the carbene carbon at 205 ppm (cf. 211 ppm in HL and 198 ppm in LiL). The ^1H NMR spectrum contains a set of resonances that can be assigned as a complex that contains three isopropoxide ligands and one NHC ligand. However, purification of **2** was hindered by the thermal instability of the complex; attempts to distill the oil at elevated temperatures under reduced pressure results in rapid decomposition, while storage under dry dinitrogen results in slow decomposition over 7 days to products that could not be identified by ^1H NMR spectroscopy.

In contrast, the treatment of a cooled (−78 °C) toluene solution of TiCl(O^{i}Pr)$_3$ with 1 equiv of **1** as a suspension in toluene results in an immediate color change of the solution to yellow, followed by the formation of a colorless precipitate over 18 h as the suspension is allowed to warm to room temperature. After filtration and removal of volatiles from the filtrate under reduced pressure, the resulting yellow oil was dissolved in diethyl ether and cooled (5 °C) to afford a crop of yellow crystals characterized as TiBr(L)(O^{i}Pr)$_2$, **3**, formed in 30% yield, Scheme 2. The high-frequency resonance at 187 ppm in the $^{13}C\{^1H\}$ NMR spectrum of **3** is attributed to the carbene C atom; the ^1H NMR spectrum of the yellow crystals shows a product containing two isopropoxide ligands for each NHC ligand. Further characterization by EI mass spectrometry showed only unassignable fragments, but the quantitative formation of **3** was confirmed by multinuclear NMR spectroscopy, elemental analysis, and single-crystal X-ray crystallography, Figure 1. These results demonstrate that the anticipated metathesis of the chloride ligand for L occurs and is associated with a ligand redistribution process in which lithium bromide is eliminated from the reaction with **1** with the metal-containing precursor. There is only one precedent for this additional halide incorporation reaction resulting from the use of a lithium bromide adduct of LiL in this chemistry. This occurs in the transamination reaction between [LiL]·LiBr and Ce(N{SiMe$_3$}$_2$)$_3$, which affords [Ce(L)(N{SiMe$_3$}$_2$)(μ-Br)]$_2$ rather than Ce(L)(N{SiMe$_3$}$_2$)$_2$.[16] The treatment of a stirred sample of **2** in toluene with stoichiometric lithium bromide for 18 h at room temperature affords a benzene-soluble solid characterized by ^1H NMR spectroscopy as **3**.

The lithium salt of L may also be isolated as [LiL]·2LiBr, **1a**. Solid TiCl(O^{i}Pr)$_3$ was mixed with **1a**, upon which a color change to yellow in the solid state was observed. Thf was added and the solution stirred overnight to afford a yellow slurry. The volatiles were removed under reduced pressure, and the yellow residue was recrystallized from cooled (5 °C) diethyl ether to afford **4** as a yellow powder, Scheme 2. The complex **4** has poor solubility in d_6-benzene; the ^1H NMR spectrum of a d_5-pyridine solution shows a 1:1 ratio of NHC:isopropoxide ligands, and the characterization of **4** as TiBr$_2$(L)(O^{i}Pr) is confirmed by elemental analysis.

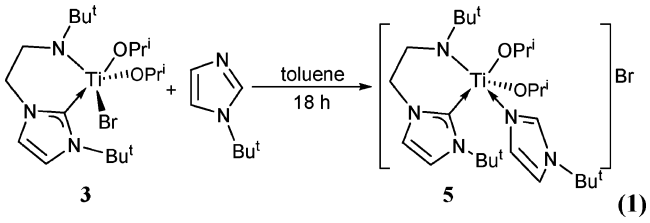

Two separate crops of single crystals of **3** suitable for X-ray diffraction were grown from a cooled solution of diethyl ether. The first crystal examined contains two independent molecules of titanium carbene **3** in the asymmetric unit. The second crystal examined also contains two independent titanium carbene molecules; one is the complex **3**, and the other is the salt [Ti(L)(CN^{t}BuCHCHN)(O^{i}Pr)$_2$]Br, **5**, in which the bromide has been displaced by an adventitious molecule of *tert*-butylimidazole. The second crystal also contains two molecules of diethyl ether lattice solvent. Complex **5** was also made independently by stirring a solution of **3** with *tert*-butylimidazole in toluene, eq 1. Thus, the imidazole molecule is either a fragment carried through from the carbene ligand synthesis or a decomposition product. The structures of the four different molecules from the two datasets, labeled A−D, are shown in Figure 1, with selected distances and angles in Table 2.

Within A and B, the metal centers are approximately square-pyramidal geometries (rather than the anticipated trigonal bipyramidal), with the N3/N3a as the apical atom for both molecules. All metal-bound ligand atoms except the N$_{amido}$ nitrogen in A and B are almost coplanar: root-mean-square (rms) deviation from the plane for molecule A is 0.034 Å and 0.0023 Å for molecule B; the Ti atom is 0.44 Å out of the plane for both A and B, and the Ti−N(3) bond is about 7.5° off perpendicular to the basal plane in both molecules. For C, the rms deviation from the analogous plane is 0.117 Å, and the Ti atom is 0.46 Å from the plane. For D, the rms deviation from the plane is 0.068 Å, and the Ti atom is 0.42 Å from the plane. The assignment of sbp geometry is least clear for D.

The Ti−C$_{carbene}$ bonds, Ti(1)−C(1) [2.252(3) Å] and Ti(2)−C(1A) [2.256(3) Å], fall within the range of reported

(31) Edworthy, I. S.; Rodden, M.; Mungur, S. A.; Davis, K. M.; Blake, A. J.; Wilson, C.; Schröder, M.; Arnold, P. L. *J. Organomet. Chem.* **2005**, *690*, 5710.

(32) Arduengo, A. J.; Tamm, M.; Calabrese, J. C.; Davidson, F.; Marshall, W. J. *Chem. Lett.* **1999**, 1021−1022.

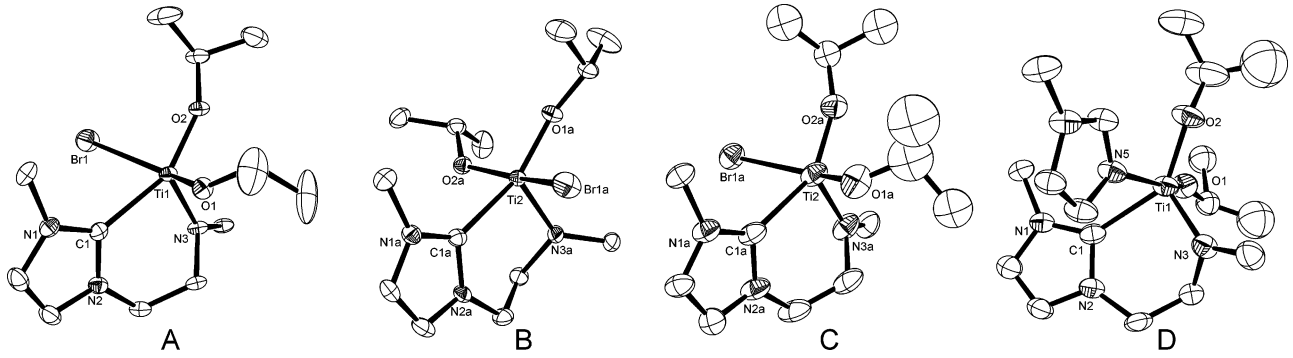

Figure 1. Displacement ellipsoid drawing of **3** (A−C) and **5** (D) (50% probability). Hydrogens, *tert*-butyl methyl groups, the bromide counterion for D, and lattice diethyl ether solvent molecules in C/D are omitted for clarity.

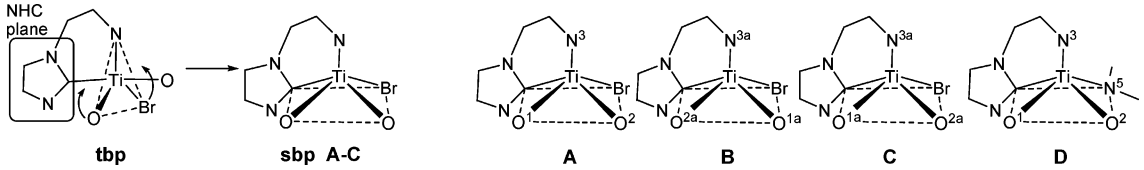

Figure 2. Diagram of the distortion trends in the core geometries of the molecular structures of **3** (A to C) and **5** (D) from the two single-crystal structure determinations of **3**.

Table 2. Selected Distances (Å) and Angles (deg) for the Three Molecules of 3 (A−C) and that of 5 (D) in the Two Crystal Structures (imz = *tert*-butylimidazole)

bond	A		B		C		D	
$Ti-C_{carbene}$	Ti1 C1	2.252(3)	Ti2 C1A	2.256(3)	Ti2 C1A	2.241(6)	Ti1 C1	2.221(6)
$Ti-N_{amide}$	Ti1 N3	1.892(3)	Ti2 N3A	1.894(3)	Ti2 N3A	1.886(6)	Ti1 N3	1.877(5)
Ti−Br	Br1 Ti1	2.6779(8)	Br1A Ti2	2.6519(7)	Ti2 Br1A	2.6985(14)		
$Ti-O_{cis}$	Ti1 O1	1.836(2)	Ti2 O2A	1.845(2)	Ti2 O1A	1.823(5)	Ti1 O1	1.791(4)
$Ti-O_{trans}$	Ti1 O2	1.792(2)	Ti2 O1A	1.790(2)	Ti2 O2A	1.790(5)	Ti1 O2	1.840(5)
$N_{carbene}-C_{carbene}$	N1 C1	1.358(4)	N1A C1A	1.363(4)	N1A C1A	1.342(8)	N1 C1	1.351(7)
							Ti1 N5 (imz)	2.265(5)
$C_{carbene}-Ti-N_{amide}$	N3 Ti1 C1	93.19(12)	N3A Ti2 C1A	93.80(12)	N3A Ti2 C1A	94.6(2)	N3 Ti1 C1	93.7(2)
$C_{carbene}-Ti-$ Br	C1 Ti1 Br1	80.25(8)	C1A Ti2 Br1A	78.43(8)	Br1A Ti2 C1A	81.42(16)		
$C_{carbene}-Ti-O_{cis}$	O1 Ti1 C1	84.45(11)	O2A Ti2 C1A	85.98(11)	O1A Ti2 C1A	86.2(2)	O1 Ti1 C1	93.2(2)
$N-C_{carbene}-N$	N1 C1 N2	104.1(3)	N2A C1A N1A	103.9(3)	N1A C1A N2A	104.1(5)	N1 C1 N2	104.1(5)
							C1 Ti1 N5 (imz)	76.8(2)

bond lengths for Ti−NHC complexes (literature mean = 2.219 Å, shortest = 2.194 Å).[1,20]

The average bite angle of the NHC ligand in **3** and **5** is 93.80°, which compares with angles of 97.57(16)° and 84.64(5)° in the tetrahedral [HL]LiBr and Sm(L)(N{$SiMe_3$}$_2$)$_2$[14] and 80.80(8)° in the dimeric, five-coordinate, [Ce(L)(N{$SiMe_3$}$_2$)(μ-Br)]$_2$.[16] The $Ti-N_{amide}$ bond lengths are typical for dialkylamido titanium species (literature mean = 1.895 Å).[33−36]

Noting the potential for a stabilizing interaction between an NHC group and a *cis*-coordinated chloride at some d^0 metal cation complexes described above,[9] we were interested to determine whether the bromide ligand might display a similar interaction with the NHC group. In addition, a potential competitor π-donor alkoxide ligand is *cis* to the bromide ligand in structures A−D.

In a five-coordinate d^0 metal complex, the geometry that corresponds to a minimum interelectron repulsion is a trigonal bipyramidal (tbp) arrangement of ligands, which is measured for the majority of five-coordinate Ti(IV) complexes reported,[36] while lower-symmetry complexes in the database contain polydentate or very bulky ligands. Since the bite angle of the unstrained ligand L is about 90°, it is reasonable to place N3/N3A and the carbene in an axial and an equatorial site of a square-based pyramid or trigonal bipyramid.

The structures are all closer to square-based pyramids (sbp) than tbp. This could suggest that a *cis*-ligand interaction occurs here too, between the carbene carbon and the isopropoxide and bromide. Figure 2 depicts the four molecules identified from the crystal structures in sbp-based geometries, showing how for molecules A−C this could arise from the two π-donor ligands, bromide and isopropoxide, occupying both sites *cis* to and normal to the carbene plane, bent toward the carbene carbon in order to generate orbital overlap with the formally empty carbenic carbon 2p orbital. The bound imidazole in D exhibits a similar bend toward the NHC group, but the two π-systems (imidazole and carbene) are not in an orientation that could facilitate a delocalization of electron density.

For the molecules A, B, and C, the $C_{carbene}-Ti-Br$ angle bisects the NHC plane, with a mean value of 80°, significantly below the value of 90° that would be expected for a square-based pyramidal structure. The other $C_{NHC}-Ti-O^iPr_{cis}$ angle in A−C averages 85.5°. (For D the angles are $C_{NHC}-Ti-O^iPr_{cis}$ = 93.2(2)°, and 76.8(2)° for $C_{NHC}-Ti-N_{imz}$.) These geometries compare to those in Ti(NMe_2)$_2$(C{NMesCH}$_2$)Cl_2, **R** (see Chart 1), in which $C_{NHC}-Ti-Cl$ (mean) = 83.35°,[20] and those in V(O)Cl_3(C{NMesCH}$_2$), in which $C_{NHC}-V-Cl_{cis}$ (mean) = 81.62°.[9] Thus, the bromide and isopropoxide ligands

(33) Novak, A.; Blake, A. J.; Wilson, C.; Love, J. B. *Chem. Commun.* **2002**, 2796.
(34) Thorn, D. L.; Nugent, W. A.; Harlow, R. L. *J. Am. Chem. Soc.* **1981**, *103*, 357.
(35) Wang, H.; Wang, Y.; Li, H.-W.; Xie, Z. *Organometallics* **2001**, *20*, 5110.
(36) Allen, F. H. *Acta Crystallogr., B* **2002**, *58*, 380−388.

Table 3. Comparison of Geometry-Optimized Data for 3 with X-ray Experimental Data

bond		X-ray	optimized
$Ti-C_{carbene}$	Ti1 C1	2.252(3)	2.294
$Ti-N_{amide}$	Ti1 N3	1.892(3)	1.933
Ti−Br	Br1 Ti1	2.6779(8)	2.710
$Ti-O_{cis}$	Ti1 O1	1.836(2)	1.874
$Ti-O_{trans}$	Ti1 O2	1.792(2)	1.824
$N_{carbene}-C_{carbene}$	N1 C1	1.358(4)	1.367
$C_{carbene}-Ti-N_{amide}$	N3 Ti1 C1	93.19(12)	93.32
$C_{carbene}-Ti-$ Br	C1 Ti1 Br1	80.25(8)	78.43
$C_{carbene}-Ti-O_{cis}$	O1 Ti1 C1	84.45(11)	85.87
$N-C_{carbene}-N$	N1 C1 N2	104.1(3)	104.2

that are *cis* to the NHC in A−D are similarly close to, and aligned with, the carbenic carbon p orbital.

The $C_{carbene}-O$ distances are 2.765, 2.792, 2.813, and 2.931 Å for A, C, B, and D, respectively; on average they are 0.43 Å within the sum of the van der Waals radii for C and O (3.22 Å). The $C_{carbene}-Br$ distances are 3.118, 3.194, and 3.240 Å for B, A, and C, respectively, on average 0.366 Å within the sum of the van der Waals radii for C and Br (3.55 Å). In the complex $[V(O)Cl_3(C\{NMesCH\}_2)]$[9] the $C_{carbene}-Cl$ distances are 2.849 and 2.887 Å, short relative to the sum of the van der Waals radii for C and Cl (3.45 Å).

However, an equally acute angle is observed in the halide-free molecule D. In the solid-state structure of **5** (D), the angle analogous to $C_{carbene}-Ti-Br$, i.e., C1−Ti1−N5, is 76.8°, equally acute, and the $C_{carbene}-N_{imz}$ distance is 2.785 Å, shorter than the van der Waals sum for C and N (3.25 Å). However, there is no clear geometric relationship between the imidazole and the NHC that would indicate an orbital interaction. The dihedral angle between the two ligand planes, that of the NHC and that of the *tert*-butyl imidazole, is 65.9°.

The distortion toward the carbene of the two *cis*-ligands could be the result of sterics if the NHC N-*tert*-butyl group were pushing into the space between the bromide and *cis*-alkoxide group, forcing them into the plane perpendicular to the carbene. However, inspection of a space-filling model of **3** suggests that both the NHC-bound N-*tert*-butyl group and isopropoxide groups have no significant hindrance to free rotation.

Theoretical Calculations

4.1. Theoretical Calculations. We have performed DFT calculations on **3** to gain insight into its electronic structure and to investigate the origin of the short $C_{carbene}\cdots Br$ and $C_{carbene}\cdots O_{alkoxide}$ distances in the solid-state structure of this compound. The crystal structures of **3** display $C_{carbene}\cdots Br$ (3.1−3.2 Å) and $C_{carbene}\cdots O_{alkoxide}$ (2.7−2.9 Å) distances and $C_{carbene}-Ti-Br$ [78.43(8)−81.42(16)°] and $C_{carbene}-Ti-O_{alkoxide}$ [84.45(11)−86.2(2)°] bond angles that suggest an interaction may exist between these π-donor ligands and the NHC π-system. Orbital overlaps between the Cl 3p orbitals and the NHC π-system in complex **R** have been used to rationalize the short $C_{carbene}\cdots Cl$ (ca. 3.1 Å) distances and acute $C_{carbene}-Ti-Cl$ bond angles (ca. 83°) extant in **R**.[20] In addition, DFT calculations have shown that the short $C_{carbene}\cdots Cl$ (ca. 3.1 Å) distances in $VOCl_3$(carbene) may arise from indirect interactions between the NHC π-system and the *cis*-coordinated chlorides, mediated by the metal d orbitals.[9]

There is excellent agreement between the metrical parameters for the experimental and geometry-optimized structures of **3**, Table 3, that suggests that the DFT calculations are of sufficient quality to permit a qualitative understanding of the electronic structure of **3**.

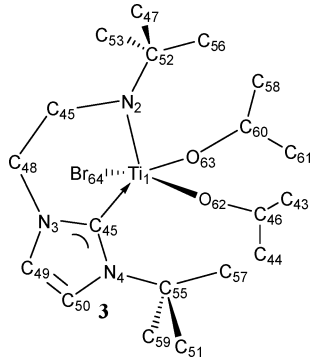

Figure 3. Atom labeling for the geometry optimization calculation for **3**.

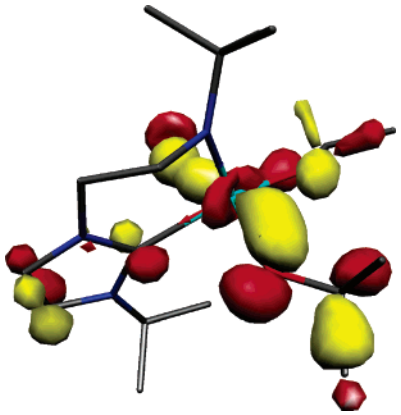

Figure 4. Isosurface for Kohn−Sham orbital 68A at the 0.05 e $Å^{-3}$ level. The red arrow along the Ti−C bond shows the *x*-axis of the Cartesian coordinate axes defined in the geometry optimization calculations; the *z*-axis is aligned with the $Ti-N_{amide}$ bond.

We have examined the molecular orbital manifold for the DFT-calculated structure of **3** and were unable to identify any direct interactions between orbitals that contain $C_{carbene}$ 2p and Br 4p character and only one orbital involving the π-system of the NHC, the 2p orbitals of the alkoxide O-donors, and the 4p orbital of the Br ligand, Figure 4. The principal interactions in this orbital involve pseudo-σ-bonding contributions between the metal 3d orbitals (14.6% metal 3d orbital character) and the Br 4p orbitals (10.5% Br 4p character), and the 2p orbitals of the *cis* (21.2% O 2p character) and *trans* (5.4% O 2p character) alkoxide ligands with only a small π-contribution (5.1%) made by the out-of-plane $C_{carbene}$ 2p orbital.

The lack of any appreciable direct orbital interaction between the ligand fragments is supported by a Wiberg bond order analysis[27] that reveals bond orders of 0.02 and 0.02−0.00 between the NHC and Br(64) and between the NHC and alkoxide fragments [defined by O(62) and O(63)], respectively. The total bond order from the Ti, Br, amide N(2), and alkoxide fragments to the NHC unit is 0.69. This is dominated by the $Ti-C_{carbene}$ interaction (Ti(1)−C(45), bond order = 0.60). For comparison, the Wiberg bond order calculated between the Ti(1) and the amide N(2) is 0.90, and for C(45)−N(3) and C(45)−N(4) of the NHC ring the bond orders are 1.30 and 1.25, respectively.

Thus, it appears that the short $C_{carbene}\cdots Br$ and $C_{carbene}\cdots O_{alkoxide}$ distances in the solid-state structure of **3** arise from steric interactions, presumably between the lone pairs on each of the Br and alkoxide donors, rather than direct orbital overlap with the formally vacant 2p orbital on $C_{carbene}$.

4.2. Conclusions. A series of titanium(IV) complexes $Ti(L)(O^iPr)_n(Br)_{3-n}$ (n = 1−3, L = ^{t}BuNHCH$_2$CH$_2$[C{N^{t}Bu-

(CHCH)N}]) have been synthesized and characterized. Structural characterization of the monobromide complex shows a distorted square-based pyramidal geometry in the three crystallographically unique molecules; in each the two π-donor ligands *cis* to the NHC group are bent toward the carbene carbon. The distorted geometries of these molecules of **3** have been studied via an inspection of space-filling plots and via a fragment overlap analysis study using DFT methods. The combined data suggest that the bending is due to repulsions between lone pairs on the adjacent π-donor ligands in the complexes rather than an orbital interaction involving the donation of bromide or alkoxide π-electron density into the carbonic C p orbital.

Acknowledgment. The authors are grateful to the EPSRC (PLA Advanced Research Fellowship, SAM studentship, and a diffractometer), the Nuffield Foundation, and the Royal Society for funding.

Supporting Information Available: Crystal structure data in CIF format, for the two crystal structure determinations of **3** and **5**. This material is available free of charge via the Internet at http://pubs.acs.org.

OM0508839